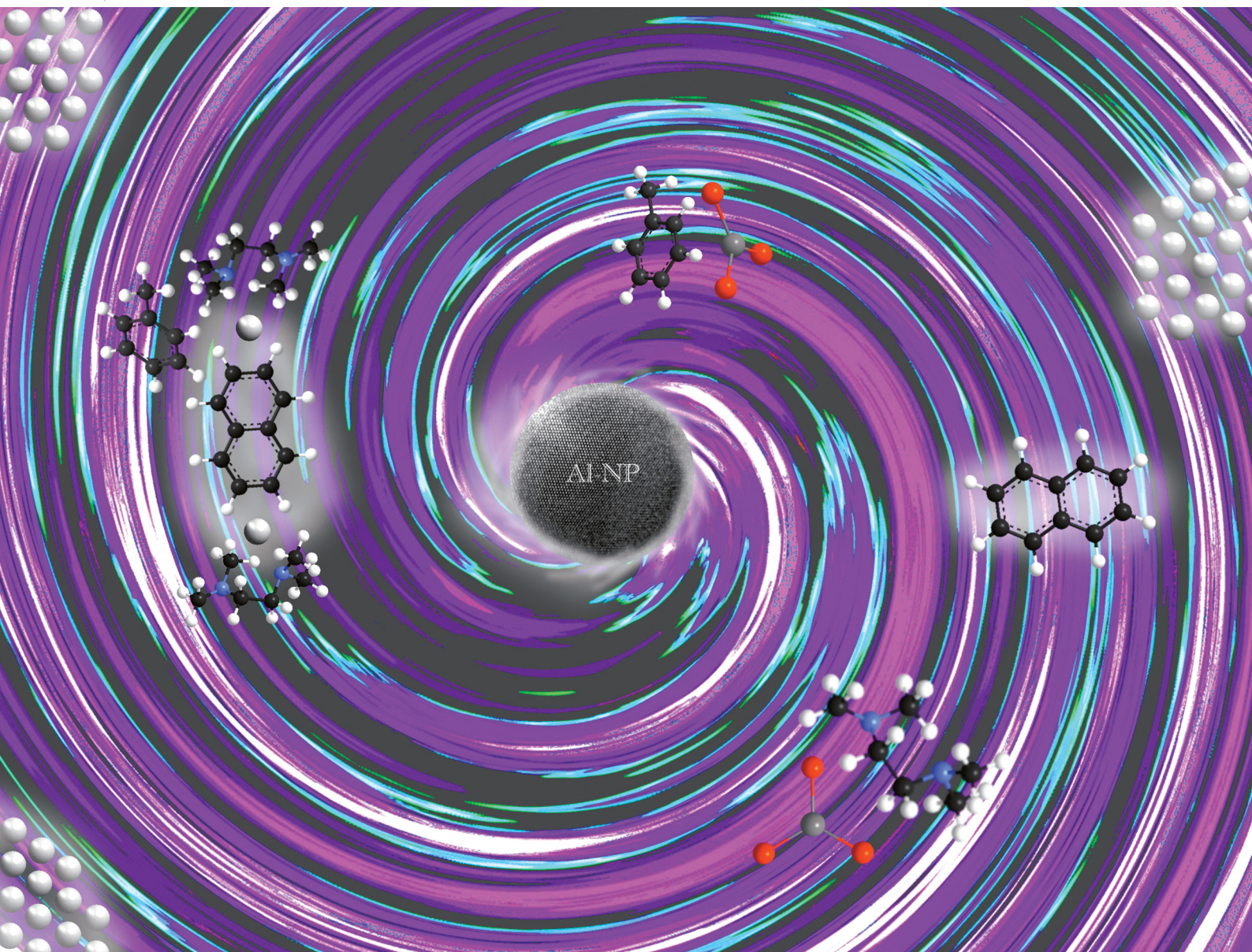


ChemComm

Chemical Communications

rsc.li/chemcomm



ISSN 1359-7345



Cite this: *Chem. Commun.*, 2022, 58, 7499

Received 31st March 2022,
Accepted 16th May 2022

DOI: 10.1039/d2cc01846b

rsc.li/chemcomm

Aluminium nanoparticles, Al(0), are obtained via liquid-phase synthesis at 25 °C. Accordingly, AlBr₃ is reduced by lithium naphthalenide ([LiNaph]) in toluene in the presence of *N,N,N',N'*-tetramethyl-ethylenediamine (TMEDA). The Al(0) nanoparticles are small (5.6 ± 1.5 nm) and highly crystalline. A light yellow colour and absorption at 250–350 nm are related to the plasmon-resonance absorption. Due to TMEDA functionalization, the Al(0) nanoparticles are colloidal and chemically stable, but show high reactivity after TMEDA removal.

Zerovalent aluminium, Al(0), nanoparticles are relevant with regard to different types of properties and applications. These include hydrogen sorption, catalysis, low-weight metals and alloys, thin-film electrodes, or high-energy materials.¹ However, the synthesis of high-purity small-sized Al(0) nanoparticles is challenging due to the high reactivity of nanosized aluminium, which can be attributed to the base character of the metal (electrochemical potential of bulk aluminium: -1.7 eV)² and the extraordinary oxophilic properties ($\Delta H_{\text{formation}} = -1677 \text{ kJ mol}^{-1}$ for the oxidation to $\alpha\text{-Al}_2\text{O}_3$).³ In contrast to bulk-Al, small-sized Al(0) nanoparticles cannot be passivated by a dense oxide layer,⁴ which is typically in a range of 4–10 nm. The high surface area and the great number of low-coordinated surface atoms increase the reactivity of Al(0) nanoparticles even further.⁵

Until now, Al(0) nanoparticles have been predominately prepared by physical methods, such as laser ablation, sputtering techniques, wire-explosion method, or ball milling.⁶ Liquid-phase methods have been rarely described. In this regard, *Haber* and *Buhro* have established a synthesis route based on AlCl₃ with LiAlH₄ forming an alane, which, thereafter, was thermally decomposed (100–160 °C) to obtain Al(0)

nanoparticles, 40–180 nm in size.⁷ This strategy has been adapted since then by several groups.⁸ Most often, aluminium particles with diameters >100 nm were obtained, often with broad size distribution and significant oxide contamination. A direct reduction of AlCl₃ in toluene/tetrahydrofuran with molten potassium or lithium naphthalenide ([LiNaph]) was introduced by Rieke *et al.*⁹ The resulting “activated aluminium” was used for C–C coupling in organic syntheses, but did not contain nanoparticles. Moreover, the naphthalenide reduction was described to be incomplete.¹⁰

Although we were recently successful with the liquid-phase synthesis of highly reactive metal nanoparticles such as the group IIIB, IVB and VB transition metals or the lanthanide metals,¹¹ the synthesis of Al(0) nanoparticles failed so far, which can be ascribed to the extraordinarily high charge density and the highly oxophilic character of Al³⁺. Thus, the reduction of AlCl₃ or AlBr₃ with lithium naphthalenide ([LiNaph]) in THF, which worked well for other base metals,¹¹ here only resulted in colourless THF complexes (at room temperature) or even a reductive cleavage of THF (above room temperature).¹²

Since ethers are chemically not stable enough as solvents for the synthesis, we have evaluated a synthesis in aromatic solvents like toluene (Tol). In this regard, AlBr₃ was used as most simple starting material being soluble in Tol. Moreover, we have selected *N,N,N',N'*-tetramethylethylenediamine (TMEDA) as an oxygen-free, aprotic ligand that may sufficiently coordinate to Al³⁺ but that may only moderately coordinate the Al(0) surface due to the steric hindrance of the methyl groups (Fig. 1). Accordingly, AlBr₃ was dissolved in Tol followed by the addition of TMEDA, which resulted in the formation of a colourless suspension of AlBr₃(TMEDA) in Tol (Fig. 1b). The composition of the AlBr₃(TMEDA) intermediate was confirmed by transmission electron microscopy (TEM), X-ray-powder diffraction (XRD), Fourier-transform infrared (FT-IR) spectroscopy, thermogravimetry (TG), and elemental analysis (EA) (Fig. S1–S4, ESI[†]). Here, it needs to be noticed that the AlBr₃(TMEDA) intermediate already forms nanoparticles with

^a Institut für Anorganische Chemie, Karlsruhe Institute of Technology (KIT), Engesserstrasse 15, 76131 Karlsruhe, Germany. E-mail: claus.feldmann@kit.edu

^b Laboratorium für Elektronenmikroskopie, Karlsruhe Institute of Technology (KIT), Engesserstrasse 7, 76131 Karlsruhe, Germany

[†] Electronic supplementary information (ESI) available: Details related to the analytical equipment, starting materials, and to the AlBr₃(TMEDA) intermediate. See DOI: <https://doi.org/10.1039/d2cc01846b>



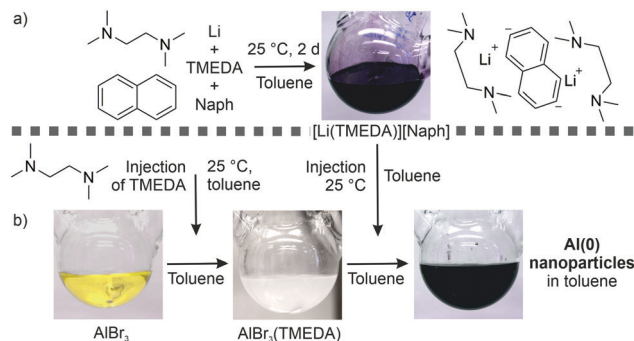


Fig. 1 Scheme illustrating the synthesis of Al(0) nanoparticles with (a) the formation of a TMEDA-stabilized [LiNaph] solution and (b) the formation of a AlBr_3 (TMEDA) suspension, in which the [LiNaph] solution was injected to obtain a black suspension of Al(0) nanoparticles.

a mean size of 9.0 ± 3.1 nm (Fig. S1, ESI†). Upon injection of [LiNaph] and TMEDA to the AlBr_3 (TMEDA) suspension in tol (Fig. 1a), $\text{Al}(0)$ nanoparticles were formed, which is indicated by the instantaneous formation of a deep black suspension (Fig. 1). TMEDA not only allows to dissolve [LiNaph] in tol but also to control the nucleation and particle size of the $\text{Al}(0)$ nanoparticles. Subsequent to synthesis, the $\text{Al}(0)$ nanoparticles were purified three times by centrifugation/redispersing in/ from tetrahydrofuran (THF) or pyridine (Py) to remove remaining starting materials and salts (e.g., naphthalene, TMEDA, LiBr). Finally, the as-prepared $\text{Al}(0)$ nanoparticles were dried in vacuum (25°C or 150°C) to obtain powder samples, or they were redispersed in Py or THF to obtain colloidally stable suspensions.‡

Scanning transmission electron microscopy (STEM) was used to examine the particle size and particle-size distribution of the as-prepared Al(0) nanoparticles (Fig. 2). According to overview images, spherical non-agglomerated nanoparticles were obtained (Fig. 2a). A mean diameter of 5.6 ± 1.5 nm with narrow size distribution was determined by statistical evaluation of > 150 nanoparticles (Fig. 2b). Considering the amount of Al in the AlBr_3 (TMEDA) intermediate, a size reduction from 9.0 ± 3.1 nm of the AlBr_3 (TMEDA) intermediate (Fig. S1, ESI[†]) to 5.6 ± 1.5 nm of the resulting Al(0) nanoparticles is in the expected range. High-resolution (HR)TEM images confirm the particle sizes and indicate the crystallinity of the as-prepared nanoparticles with a well-resolved crystalline lattice throughout the whole particle (Fig. 2c). A simulated diffraction pattern, which was generated by Fourier transformation of the HRTEM image, is well in agreement with cubic bulk aluminium with $a = 4.0495 \text{ \AA}$ in the [101] zone axis (Fig. 2d).¹³ Here, it should be also noticed that STEM and HRTEM images did not show any traces of aluminium-oxide species.

Besides selected nanoparticles on TEM images, crystallinity and surface functionalization of the as-prepared Al(0) nanoparticles were examined by X-ray powder diffraction (XRD) (Fig. 3a). The observed Bragg reflections are in agreement with bulk aluminium as a reference. Moreover, Bragg peaks of eventual impurity phases were not observed. According to a

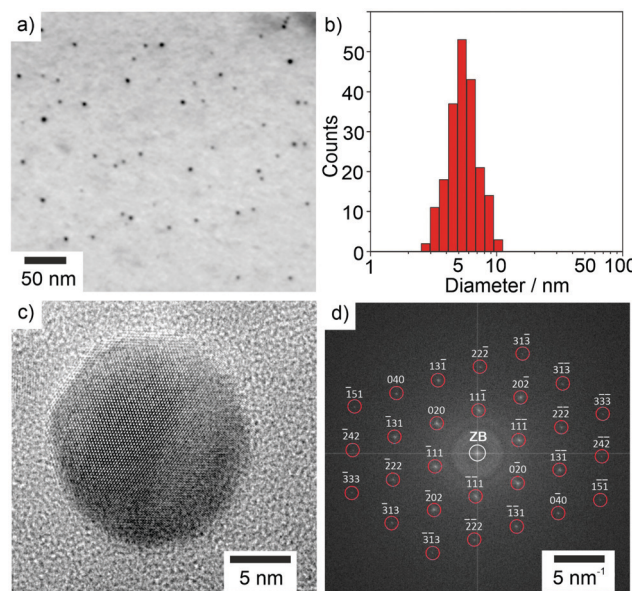


Fig. 2 Electron microscopy of the as-prepared Al(0) nanoparticles: (a) STEM overview image, (b) size distribution according to a statistical evaluation of >150 nanoparticles on STEM images, (c) HRTEM image of a selected nanoparticle with lattice fringes, and (d) FFT analysis of single nanoparticle shown in (c) (zero-order beam marked by white circle).

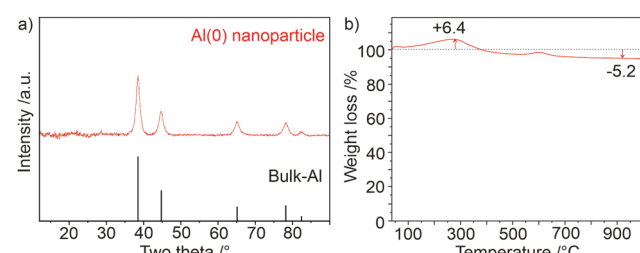


Fig. 3 Composition of the as-prepared Al(0) nanoparticles: (a) X-ray powder diffraction (bulk aluminium as a reference, ICDD-No. 00-004-0787), (b) thermogravimetry (in argon atmosphere).

Rietveld refinement, the broadening of the Bragg reflections refers to a mean crystallite size of 7.6 nm, which matches with the mean particle size obtained by electron microscopy. In addition, EA and TG were used to examine the surface functionalization. After purification by centrifugation/redispersion in/ from THF, EA indicates C/H/N contents of 24.9% C, 1.5% N, and 3.5% H. The low N-content indicates that most of the TMEDA was indeed removed by the purification process, resulting in THF as the predominate molecule adhered on the particle surface. TG analysis of THF-treated Al(0) nanoparticles shows an increase in weight (6.4%) up to a temperature of 280 °C, followed by a weight loss (in total 5.2%) up to a temperature of 1000 °C (Fig. 3b). The thermal residue was identified as Al₂O₃ *via* XRD (Fig. S5, ESI†). Thus, the weight loss due to the combustion of surface-adhered TMEDA and THF is more-or-less compensated by the weight increase of the oxidation. If the Al(0) nanoparticles were purified by

centrifugation/redispersion in/from Py, EA resulted in 39.7% C, 8.7% N and 3.5% H. The C/N-ratio of 4.6 matches with the C/N ratio of Py (5.0) and now points to Py as the predominate surface functionalization.

FT-IR spectroscopy confirms the aforementioned findings related to the surface functionalization (Fig. 4). Thus, TMEDA is adhered on the surface of the as-prepared Al(0) nanoparticles as indicated by the observed vibrations that are very comparable to pure TMEDA. Surface-adhered TMEDA can be removed by heating in vacuum (Fig. 4a) or by redispersion/centrifugation in/from suitable solvents (Fig. 4b). Accordingly, the intensity of the TMEDA-related vibrations (*i.e.*, $\nu(\text{C-H})$, $\nu(\text{N-C}_{\text{CH}_2})$, $\nu(\text{N-C}_{\text{CH}_3})$) was significantly reduced after vacuum treatment at room temperature and even further after heating in vacuum to 150 °C (Fig. 4a). In regard of the solvents, Tol, THF and pyridine were evaluated. Hereof, THF turned out to be most efficient with a significant reduction of the TMEDA-related vibrations (Fig. 4b).

Suspensions of the as-prepared Al(0) nanoparticles in THF (0.2–0.5 wt%) are colloidally stable for several weeks without agglomeration or oxidation. Interestingly, these suspensions show a yellowish colour, which is especially noticeable when illuminated with a strong white-light source (*e.g.* halogen lamp with glass fibre, Fig. 5a). This colour can be attributed to the Al(0) nanoparticles since a colourless supernatant is remaining after centrifugation. The findings were quantified *via* UV-Vis spectroscopy (Fig. 5b). Here, the yellow colour can be related to a specific absorption at 250–350 nm. Such shift of the plasmon resonance into the visible due to quantum confinement is often observed for very small metal particles with gold as the most prominent example¹⁴ and was also described in the ultraviolet to blue spectral range for Al(0) nanoparticles.^{8c,15} Here, it must be noticed that the exact wavelength position of the plasmon-resonance absorption not only depends on the particle size but also on the specific surface functionalization. In fact, the plasmon-resonance absorption of Al(0) nanostructures was already used for sensing as well as to enhance the light absorption of silicon.¹⁶ However, these Al(0) nanostructures were yet typically established *via* gas-phase deposition or reduction of Al₂O₃ nanoparticles, and they exhibit sizes of 10 to 100 nm.^{15,16}

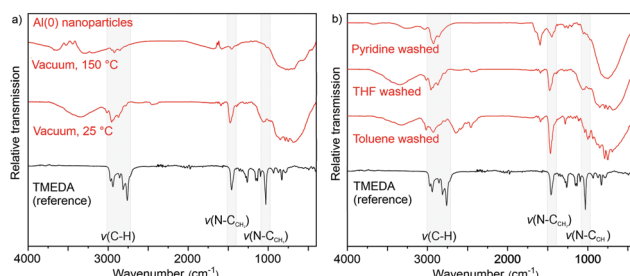


Fig. 4 Surface functionalization of the Al(0) nanoparticles: (a) vacuum treatment, (b) redispersion/centrifugation in/from different solvents (with TMEDA as a reference and selected vibrations as indicators).

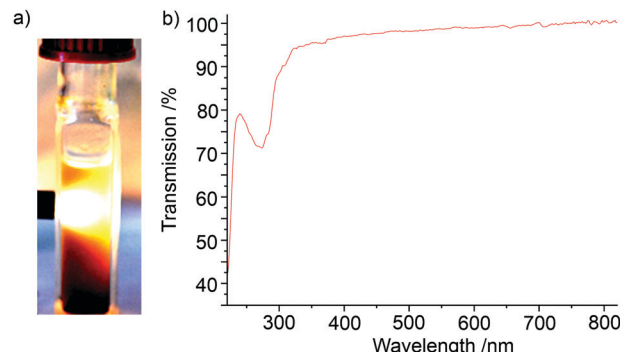


Fig. 5 Optical properties of Al(0) nanoparticles: (a) suspension in THF, (b) UV-Vis spectrum.

Finally, the reactivity of the Al(0) nanoparticles was evaluated. Interestingly, the as-prepared nanoparticles with TMEDA surface termination are stable in air (Fig. 6a). After heating in vacuum to 150 °C, however, Al(0) powder samples become highly reactive and show instantaneous ignition when in contact to air (Fig. 6a). This finding is in agreement with FT-IR spectra that indicate a removal of surface-adhered TMEDA after heating to 150 °C. In contrast, the as-prepared Al(0) nanoparticles show direct reaction with water (Fig. 6b). Thus, addition of water to a nanoparticle suspension in THF resulted in the formation of H₂ after 5–10 seconds and total decolourisation of the suspension within some minutes. This behaviour also confirms the absence of aluminium oxide passivation layers on the as-prepared Al(0) nanoparticles, which would otherwise be non-reactive after heating as well as upon addition of water.⁴ In sum, this also gives the opportunity to control the reactivity of the Al(0) nanoparticles with low reactivity in the presence of the TMEDA surface functionalization and high reactivity after the removal of the surface-adhered TMEDA.

In summary, aluminium nanoparticles, Al(0), were obtained *via* room-temperature liquid-phase synthesis in toluene. AlBr₃ was reduced by lithium naphthalenide ([LiNaph]) without the

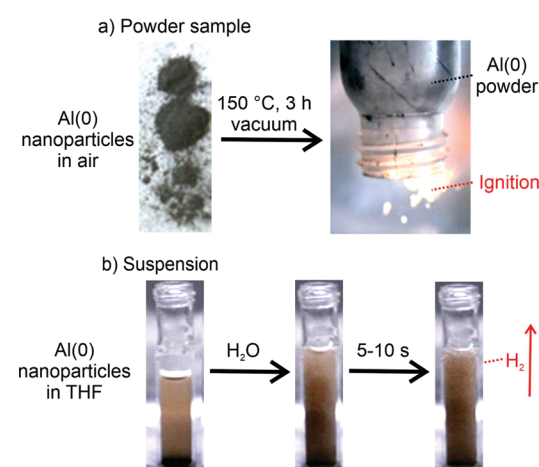


Fig. 6 Reactivity of the as-prepared Al(0) nanoparticles: (a) powder sample in contact to air prior and after heating (150 °C, 3 h), (b) suspension in THF prior and after addition of water.



need for the widely used alane-type precursors. *N,N,N',N'-tetramethylethylenediamine* (TMEDA) was used to make [LiNaph] soluble in toluene, to control nucleation and size, and to guarantee the colloidal and chemical stability of the Al(0) nanoparticles. The as-prepared Al(0) nanoparticles exhibit unprecedented small-size (5.6 ± 1.5 nm), narrow size distribution, and high crystallinity ($a = 4.0495$ Å). A light yellow colour (absorption at 250–350 nm) can be related to the plasmon-resonance absorption. TMEDA as a surface functionalization can be removed from the particle surface by heating (vacuum, 150 °C) or by washing with pyridine or THF, which also allows to influence the reactivity of the Al(0) nanoparticles (no reaction in air in the presence of TMEDA; spontaneous ignition after removal of TMEDA). The new synthesis strategy (e.g., simple aluminium halides as starting materials, TMEDA for stabilization) and the high particle quality in terms of size, size distribution, and crystallinity open up new perspectives for application (e.g., H₂ sorption, catalysis, low-weight metals, high-energy materials).

The authors are grateful to the Deutsche Forschungsgemeinschaft (DFG) for funding of personnel (NanoMet: FE911/11-1, GE 841/29-1) and TEM equipment (INST 121384/33-1 FUGG).

Conflicts of interest

There are no conflicts to declare.

Notes and references

‡ Experimental. [LiNaph] solution. 42 mg (6 mmol) of lithium were added to a solution of 400 mg (3.1 mmol) of naphthalene in 80 mL of Tol. 1 mL (6.6 mmol) of TMEDA were added to the solution with intense stirring. Here, TMEDA is required to make [LiNaph] soluble in Tol. Moreover, it needs to be noticed that glass-covered stirring bars need to be used since Teflon-covered stirring bars react with [LiNaph]. The formation of [LiNaph] was visibly indicated by the formation of a deep purple solution after addition of lithium. The solution was stirred for 2 days to guarantee complete dissolution of all lithium prior use. Al(0) nanoparticles. 500 mg (1.9 mmol) of AlBr₃ were dissolved in 20 mL of Tol to form a yellowish solution. 300 µL (2.0 mmol) of TMEDA were injected with intense stirring, which resulted in the formation of a colourless suspension. Thereafter, the aforementioned [LiNaph] solution was injected and instantaneously lead to a black suspension. After centrifugation (20 000×g), the Al(0) nanoparticles were resuspended/centrifuged in/from THF or pyridine to remove remaining starting materials and salts. The as-prepared Al(0) nanoparticles were redispersed in THF or dried in vacuum to obtain a dark grey powder samples.

1 (a) T. Klein, C. Pauly, F. Muecklich and G. Kickelbick, *Intermetallics*, 2020, **124**, 106839; (b) S. Elbasuney, Z. M. Gaber, M. Radwan and S. F. Mostafa, *Appl. Surf. Sci.*, 2017, **419**, 328–336; (c) W. Zhao, J. Li,

C. He, L. Wang, J. Chu, J. Qu, T. Qi and Z. Hao, *Catal. Today*, 2010, **158**, 427–431.

2 A. F. Holleman and E. Wiberg, *Anorganische Chemie*, ed., de Gruyter, Berlin, 2017, vol. 1, 103, Annex III/IV.

3 L. L. Wang, Z. A. Munir and Y. M. Maximov, *J. Mater. Sci.*, 1993, **28**, 3693–3708.

4 (a) M. J. McClain, A. E. Schlather, E. Ringe, N. S. King, L. Liu, A. Manjavacas, M. W. Knight, I. Kumar, K. H. Whitmire, H. O. Everitt, P. Nordlander and N. J. Halas, *Nano Lett.*, 2015, **15**, 2751–2755; (b) B. Ma, F. Zhao, X. Cheng, F. Miao and J. Zhang, *J. Appl. Phys.*, 2017, **121**, 145108.

5 F. Vines, J. R.-B. Gomes and F. Illas, *Chem. Soc. Rev.*, 2014, **43**, 4922–4939.

6 (a) M. Barberio, S. Giusepponi, S. Vallieres, M. Sciscio, M. Celino and P. Antici, *Sci. Rep.*, 2020, **10**, 9570; (b) N. K. Agrawal, R. Agarwal, D. Bhatia, D. Saxena, G. Kedawat, K. C. Swami and Y. K. Vijay, *Adv. Mater. Lett.*, 2015, **6**, 301–308; (c) Y. Wen and D. Xia, *Nanotechnology*, 2018, **29**, 125301; (d) A. Baladi, R. Mamoory and R. Sarraf, *Internat. J. Mod. Phys.*, 2012, **5**, 58–65; (e) Z. R. Hesabi, S. Kamrani, A. Simchi and S. M.-S. Reihani, *Powder Metall.*, 2009, **52**, 151–157; (f) C. Chazelas, J. F. Coudert, J. Jarrige and P. Fauchais, *J. Europ. Ceram. Soc.*, 2006, **26**, 3499–3507.

7 J. A. Haber and W. E. Buhro, *J. Am. Chem. Soc.*, 1998, **120**, 10847–10855.

8 (a) T. Klein and G. Kickelbick, *Dalton Trans.*, 2020, **49**, 13–19; (b) C. R. Jacobson, D. Solti, D. Renard, L. Yuan, M. Lou and N. J. Halas, *Acc. Chem. Res.*, 2020, **53**, 2020–2030; (c) B. D. Clark, C. J. De Santis, G. Wu, D. Renard, M. J. McClain, L. Bursi, A.-L. Tsai, P. Nordlander and N. J. Halas, *J. Am. Chem. Soc.*, 2019, **141**, 1716–1724; (d) M. J. McClain, A. E. Schlather, E. Ringe, N. S. King, L. Liu, A. Manjavacas, M. W. Knight, I. Kumar, K. H. Whitmire and H. O. Everitt, *Nano Lett.*, 2015, **15**, 2751–2755; (e) T. J. Foley, C. E. Johnson and K. T. Higa, *Chem. Mater.*, 2005, **17**, 4086–4091.

9 R. D. Rieke and L. Chao, *Synth. React. Inorg., Met.-Org., Nano-Met. Chem.*, 1974, **4**, 101–105.

10 L. A. Garza-Rodríguez, B. I. Kharisov and O. V. Kharissova, *Synth. React. Inorg., Met.-Org., Nano-Met. Chem.*, 2009, **39**, 270–290.

11 (a) C. Schöttle, D. Doronkin, R. Popescu, D. Gerthsen, J.-D. Grunwaldt and C. Feldmann, *Chem. Commun.*, 2016, **52**, 6316–6319; (b) A. Egeberg, L.-P. Faden, A. Zimina, J.-D. Grunwaldt, D. Gerthsen and C. Feldmann, *Chem. Commun.*, 2021, **57**, 3648–3651; (c) D. Bartenbach, O. Wenzel, R. Popescu, L.-P. Faden, A. Reif, M. Kaiser, A. Zimina, J.-D. Grunwaldt, D. Gerthsen and C. Feldmann, *Angew. Chem., Int. Ed.*, 2021, **60**, 17373–17377.

12 R. D. Rieke, *Chemical Synthesis Using Highly Reactive Metals*, Wiley, New York, 2017.

13 W. Witt, *Z. Naturforsch., A: Phys. Sci.*, 1967, **22**, 92–95.

14 (a) G. Maidecchi, G. Gonella, R. Proietti Zaccaria, R. Moroni, L. Anghinolfi, A. Giglia, S. Nannarone, L. Mattera, H. L. Dai, M. Canepa and N. Bisio, *ACS Nano*, 2013, **7**, 5834–5841; (b) C. Langhammer, M. Schwind, B. Kasemo and I. Zoric, *Nano Lett.*, 2008, **8**, 1461–1471; (c) Y. Ekinci, H. H. Solak and J. F. Löffler, *J. Appl. Phys.*, 2008, **104**, 083107.

15 (a) Y. Ekinci, H. H. Solak and J. F. Löffler, *J. Appl. Phys.*, 2008, **104**, 083107; (b) C. Langhammer, M. Schwind, B. Kasemo and I. Zoric, *Nano Lett.*, 2008, **8**, 1461–1471.

16 (a) S. Khadir, A. Diallo, M. Chakaroun and A. Boudrioua, *Opt. Exp.*, 2017, **25**, 9812–9822; (b) C. Zhao, Y. Zhu, Y. Su, Z. Guan, A. Chen, X. Ji, X. Gui, R. Xiang and Z. Tang, *Adv. Opt. Mater.*, 2015, **3**, 248–256; (c) S. K. Jha, Z. Ahmed, M. Agio, Y. Ekinci and J. F. Löffler, *J. Am. Chem. Soc.*, 2012, **134**, 1966–1969; (d) T. F. Villesen, C. Uhrenfeldt, B. Johansen, J. L. Hansen, U. H. Ulrikisen and A. N. Larsen, *Nanotechnology*, 2012, **23**, 085202.

